Conformational Changes in Actin Filaments Induced by Formin Binding to the Barbed End

Gábor Papp,* Beáta Bugyi,* Zoltán Ujfalusi,* Szilvia Barkó,* Gábor Hild,† Béla Somogyi,*† and Miklós Nyitrai*
*Department of Biophysics, Faculty of Medicine, and †Research Group for Fluorescence Spectroscopy, Office for Academy Research Groups, University of Pécs, Pécs, Hungary

ABSTRACT Formins bind actin filaments and play an essential role in the regulation of the actin cytoskeleton. In this work we describe details of the formin-induced conformational changes in actin filaments by fluorescence-lifetime and anisotropy-decay experiments. The results show that the binding of the formin homology 2 domain of a mammalian formin (mouse mDia1) to actin filaments resulted in a less rigid protein structure in the microenvironment of the Cys^{374} of actin, weakening of the interactions between neighboring actin protomers, and greater overall flexibility of the actin filaments. The formin effect is smaller at greater ionic strength. The results show that formin binding to the barbed end of actin filaments is responsible for the increase of flexibility of actin filaments. One formin dimer can affect the dynamic properties of an entire filament. Analyses of the results obtained at various formin/actin concentration ratios indicate that at least 160 actin protomers are affected by the binding of a single formin dimer to the barbed end of a filament.

INTRODUCTION

Formins are evolutionary conserved proteins with complex domain structure and play essential roles in the regulation of the dynamic organization of the cytoskeleton. Formins exert their effects in processes as diverse as cytokinesis, actin cable formation, cell polarity determination, stress fiber formation, vesicular trafficking, and stabilization of microtubules in a wide range of organisms (1–7). A common characteristic feature of the formin family of proteins is the presence of a formin homology 2 domain (FH2) that has a key role in the multiple effects of formins on actin dynamics. Cooperating with the profilin binding FH1 domain, the FH2 domain appears to play a central role in the promotion of actin assembly (8–10). It was previously established that the functional form of the FH2 domain is dimeric (10–12). mDia1-FH2 can bind tightly to the barbed end of actin filaments (10,11,13). The members of a subfamily of formins, the diaphanous related formins possess a specific diaphanous autoregulatory domain on their C-terminus and a GTPase binding domain (GBD) on the N-terminus. These domains regulate the activity of the protein. The binding of Rho-GTPases to GBD causes the release of the autoinhibitory interactions between GBD and the diaphanous autoregulatory domain, exposing the FH1 and FH2 domains (14–18).

Previous studies have provided little information regarding the effect of formins on the conformational properties of actin filaments. Based on the results of temperature-dependent fluorescence resonance energy transfer experiments, we reported recently that mDia1-FH2 induced conformational changes in the actin filaments in a formin-concentration-dependent manner. On the basis of these observations, we hypothesized that the binding of formins to the barbed end of actin filaments makes the filaments more flexible through long-range allosteric interactions, whereas at higher formin concentrations the side binding of mDia1-FH2 could stabilize the protomer-protomer interactions and stiffen the structure of the filaments (19).

In this work, we carried out time-resolved fluorescence lifetime and anisotropy decay experiments to further explore the effect of mDia1-FH2 on the dynamic and conformational properties of actin filaments. Fluorescence lifetime experiments showed that formin binding induced local conformational changes in the vicinity of Cys^{374}. Analyses of the anisotropy decay experiments corroborated our previous conclusion (19) that mDia1-FH2 makes the structure of the actin filaments more flexible. The formin effect on the actin filaments was dependent on ionic strength. The actin concentration independence of the formin effects indicated that it was the binding of formin fragments to the barbed end that loosened the filament structure by long-range allosteric effects. Based on the observations, we estimated that the binding of one mDia1-FH2 dimer could affect the conformation of at least 160 actin protomers in a filament.

MATERIALS AND METHODS

Protein preparations

The FH2 fragments of mammalian formin mDia1 (mDia1-FH2) were prepared as in Shimada et al. (11). The mDia1-FH2 fragments were expressed as glutathione transferase fusion proteins in *Escherichia coli* BL21 (DE3)pLysS strain. Transformed cells were multiplied and the protein expression was induced with isopropyl-β-D-thiogalactopyranoside. The clarified cell lysate was loaded onto a GSH column (Amersham, Buckinghamshire, UK). The separated glutathione transferase formin has

Submitted April 24, 2006, and accepted for publication June 12, 2006.

Gábor Papp and Beáta Bugyi contributed equally to this work.

Address reprint requests to Miklós Nyitrai, Dept. of Biophysics, Faculty of Medicine, University of Pécs, Pécs, Szigeti str. 12, H-7624, Hungary. Tel.: 36-72-536267; Fax: 36-72-536261; E-mail: miklos.nyitrai@aok.pte.hu.

0006-3495/06/10/2564/09 $2.00

doi: 10.1529/biophysj.106.087775

been cleaved with thrombin and eluted from the column. For further purification we used size-exclusion chromatography (Sephacryl S-300). After photometrical determination of the concentration (extinction coefficient was $\varepsilon_{280} = 21{,}680\ M^{-1}\ cm^{-1}$at 280 nm, which was estimated with ProtParam, http://us.expasy.org/tools/), the purified protein was frozen in liquid nitrogen and stored at −80°C. The formin concentrations are given as mDia1-FH2 monomer concentrations throughout this article, unless stated otherwise.

Acetone-dried powder from rabbit skeletal muscle was obtained as described earlier (20). Rabbit skeletal-muscle actin was prepared according to Spudich and Watt (21). The actin was further purified by Sephacryl S-300 column chromatography and stored in 4 mM Tris-HCl, pH 7.3, 0.2 mM ATP, 0.1 mM $CaCl_2$, 0.5 mM DTT (buffer A). Before the fluorescence measurements, the actin monomer (G-actin) solution was clarified by a 1-h ultracentrifugation at 100,000 × *g*. Concentration of G-actin was determined spectrophotometrically with the absorption coefficient of 0.63 $mg^{-1}\ ml\ cm^{-1}$ at 290 nm (22), using a Shimadzu UV-2100 spectrophotometer. Relative molecular weight of 42,300 was used for G-actin (23).

Actin was labeled with IAEDANS at Cys^{374} (Fig. 1), according to Miki and co-workers (24). The concentration of the fluorescence dye in the protein solution was determined using the absorption coefficient of 6100 $M^{-1}\ cm^{-1}$ at 336 nm for IAEDANS bound to actin (25). The extent of labeling was determined by photometry and was found to be 0.8–0.9 mol/mol of actin monomer.

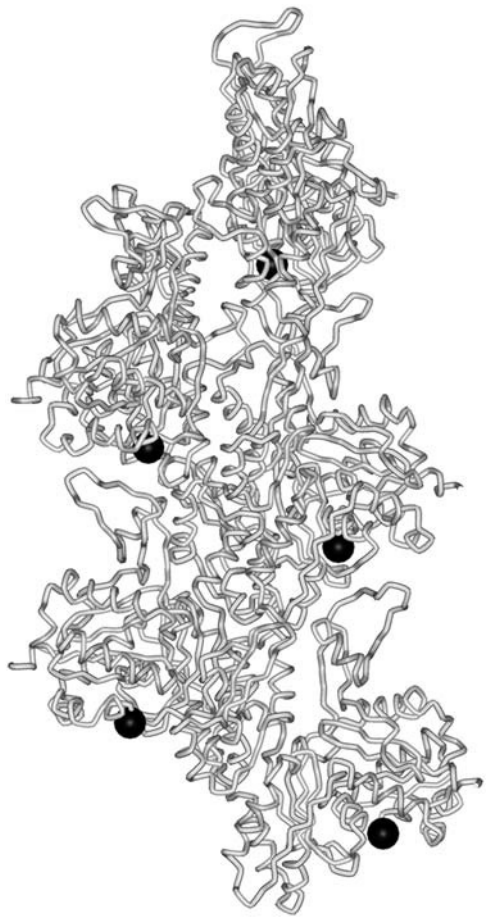

FIGURE 1 Schematic representation of an actin filament. The tube representation shows five actin monomers in a filament. Dark circles indicate the approximate position of the Cys^{374} residue, which was labeled in this study with a fluorescence probe.

Before the polymerization of actin, Mg-G-actin was prepared from Ca-G-actin by the addition of EGTA and $MgCl_2$ to the final concentrations of 0.2 mM and 0.05 mM, respectively, and the solution was incubated for 10 min at room temperature.

Fluorescence lifetime and anisotropy decay measurements

Samples were prepared by mixing Mg-G-actin and mDia1-FH2 to establish the desired protein concentrations. The samples were polymerized by the addition of $MgCl_2$ and KCl to the final concentrations of 0.5 mM and 10 mM, unless stated otherwise. The samples of actin filaments and formin were incubated overnight at 4°C before the fluorescence experiments. Fluorescence lifetime and emission anisotropy decay were measured at 22°C with an ISS K2 multi-frequency phase fluorometer (ISS Fluorescence Instrumentation, Champaign, IL) using the frequency cross-correlation method. The measurements were carried out in a thermostated sample holder. The temperature was maintained using a HAKE F3 water bath. The excitation light source was a 300 W Xe arc-lamp and the excitation light intensity was modulated with a double-crystal Pockels cell. Excitation wavelength was set to 350 nm and the emission was monitored through a 385FG0325 high-pass filter. The phase delay and the demodulation of the sinusoidally modulated fluorescence signal were measured with respect to the phase delay and the demodulation of a standard reference substance. Freshly prepared glycogen solution was used as a reference (lifetime = 0 ns). In anisotropy decay measurements the sample was excited with polarized light. The fluorescence lifetimes and rotational correlation times were determined using nonlinear least-square analysis carried out with the ISS187 decay analysis software. The goodness of fit was determined from the value of the reduced χ^2.

In fluorescence lifetime measurements all data were fit to double-exponential decay curves or to a unimodal Gaussian distribution, assuming a constant, frequency-independent error in both phase angle (±0.200°) and modulation ratio (±0.004). In double-exponential lifetime analyses the average fluorescence lifetimes were calculated as

$$\tau_{aver} = (\tau_1\alpha_1 + \tau_2\alpha_2)/(\alpha_1 + \alpha_2), \quad (1)$$

where τ_{aver} is the average fluorescence lifetime, and α_i and τ_i are the individual amplitude and lifetime, respectively.

The anisotropy is expected to decay as a sum of exponentials (26). The row data were fitted to a double exponential function:

$$r(t) = r_1 \exp(-t/\phi_1) + r_2 \exp(-t/\phi_2), \quad (2)$$

where ϕ_1 and ϕ_2 are the two rotational correlation times with amplitudes r_1 and r_2, respectively. The limiting anisotropy recovered at zero time is given by

$$R_0 = r_1 + r_2. \quad (3)$$

The two-dimensional angular range of the cone, Θ, within which the fluorophore performs wobbling motion can be related to the amplitudes of the two rotational modes resolved in anisotropy decay measurements (27):

$$(r_1/(r_1 + r_2)) = (\cos^2\Theta(1 + \cos\Theta)^2)/4. \quad (4)$$

Here, r_1 is the amplitude of the slower of the two exponential decay components.

RESULTS

The effect of mDia1-FH2 on the fluorescence lifetime of IAEDANS-actin

Fluorescence probes attached to proteins can reflect the conformational changes in their microenvironment. In our

experiments, the fluorescence lifetime of IAEDANS attached to Cys^{374} was investigated to characterize the effect of mDia1-FH2 on the structure of actin filaments. In these measurements, 20 μM actin was polymerized in the presence of various concentrations of mDia1-FH2 (0–5 μM). The modulation and phase data were obtained between 5 MHz and 80 MHz (Fig. 2 *A*). The analyses of the fluorescence lifetime measurements were carried out using one-, two-, or three-exponential decay models. The double-exponential analyses (χ^2 = 1–3) gave better fits than the single-exponential fits (χ^2 = 6–12). When the sum of three exponentials was used, the goodness of the fit did not improve as compared to the double-exponential fits, indicating that the assumption of two exponential decay components gave the best description of the physically veritable lifetimes. The experimental data were analyzed assuming unimodal Gaussian lifetime distributions as well, which also proved to be a powerful tool in the analyses of fluorescence lifetime measurements (28–31). The average lifetimes from double-exponential analyses (τ_{aver}) (Eq. 1) and the mean fluorescence lifetimes from Gaussian analyses were used for the interpretation of the fluorescence lifetime results.

Both types of analyses showed that the fluorescence lifetime of IAEDANS decreased from ~20 ns in the absence of formins to ~18.5 ns in the presence of mDia1-FH2 (Fig. 2 *B*). The decrease of the fluorescence lifetime was formin-concentration-dependent below 500 nM mDia1-FH2 and became formin-concentration-independent above this concentration. The effect of formin on the fluorescence lifetimes indicated that the binding of mDia1-FH2 modified the microenvironment of the Cys^{374} in actin filaments.

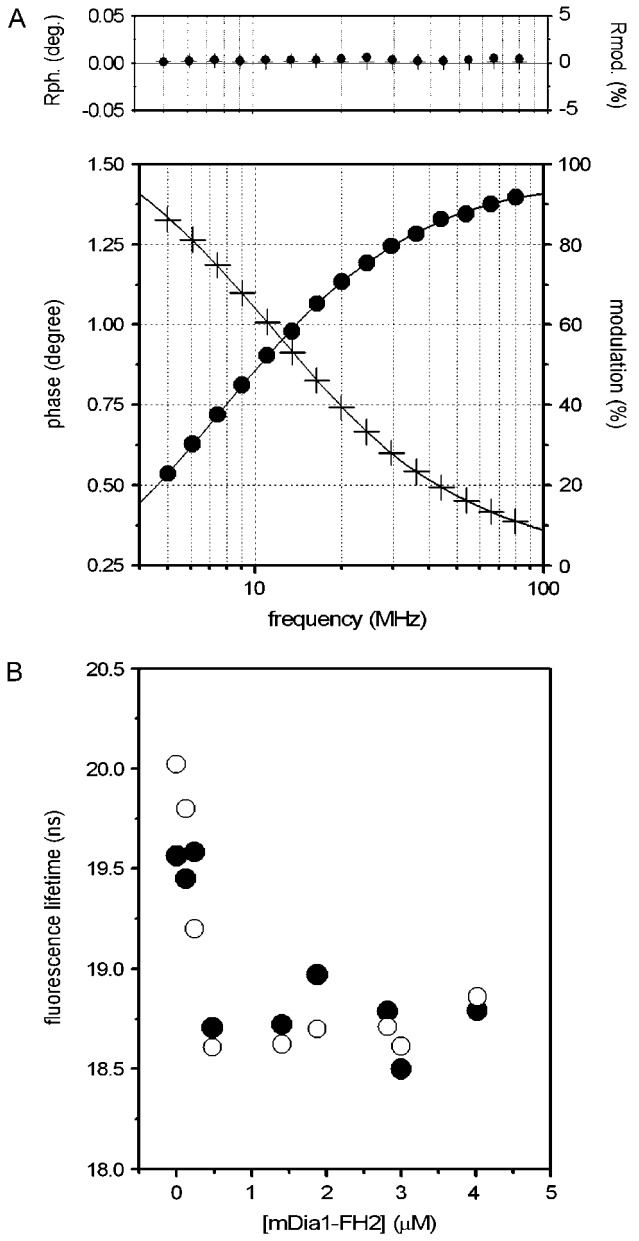

FIGURE 2 mDia1-FH2 affects the fluorescence lifetime of IAEDANS-actin filaments. (*A*) The frequency-dependent phase (*solid circles*) and modulation (*crosses*) data from fluorescence lifetime experiments with 20 μM actin in the absence of formin. Solid line indicates the results from double-exponential fits. The upper panel shows the differences between the measured values and those calculated from the nonlinear least-square analyses. (*B*) The mDia1-FH2 concentration dependence of the fluorescence lifetime measured at 20 μM actin. The figure shows the average lifetimes (*solid circles*) from double-exponential fits and the mean lifetimes (*open circles*) from Gaussian analyses. The experiments were carried out at 0.5 mM $MgCl_2$ and 10 mM KCl.

The effect of mDia1-FH2 on the dynamic properties of actin filaments

The difference in the local conformation of the protein matrix around Cys^{374} could reflect the modification of a larger segment or the entire actin filament. Our previous study indicated that such larger-scale formin-induced conformational changes were present in actin filaments (19). To further characterize the formin-induced conformational changes in actin filaments the anisotropy decay of the IAEDANS-actin filaments was measured between 2 MHz and 100 MHz. The obtained frequency-dependent phase and modulation data were analyzed with double-exponential fits (Eq. 2)(26). In these analyses, two rotational correlation times were determined. We attributed the shorter rotational correlation time (ϕ_2) to the motion of the probe relative to the protein, but the longer one (ϕ_1) to the motion of the protein matrix. The former one ranged between 2 ns and 4 ns in our experiments and showed little formin-concentration dependence (Fig. 3 *A*, *inset*). The longer rotational correlation time was ~700 ns in the absence of formin, similar to that observed in previous works (32,33). The value of this parameter decreased to ~100 ns in the presence of 500 nM mDia1-FH2 and remained formin-concentration-independent above this concentration (Fig. 3 *A*). Previously it was established that the value of the longer correlation time is inversely proportional to the flexibility of the actin filaments (32,34–37). Therefore, the formin-induced decrease of the rotational correlation

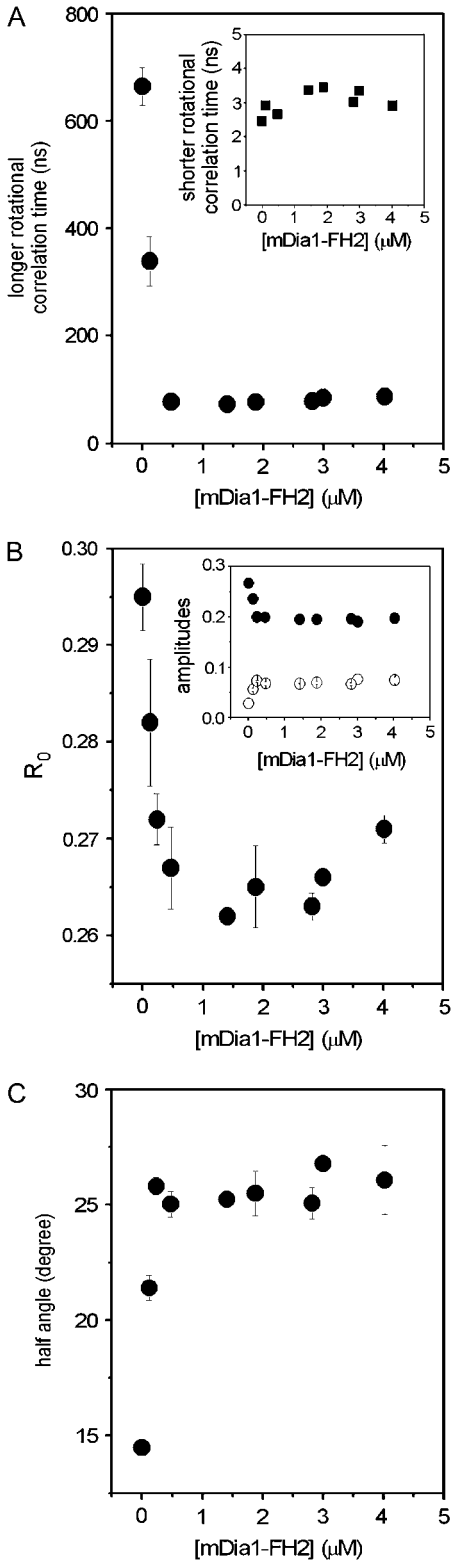

FIGURE 3 mDia1-FH2 influenced the anisotropy decay of IAEDANS-actin filaments. (*A*) The mDia1-FH2 concentration dependence of the longer rotational correlation times measured at 20 μM actin. (*Inset*) Values of the shorter rotational correlation times as a function of [mDia1-FH2]. (*B*) The formin dependence of the limiting anisotropy values determined from anisotropy decay experiments. (*Inset*) Formin dependence of the amplitudes of the shorter (*open circles*) and longer (*solid circles*) rotational correlation times. (*C*) The mDia-FH2 concentration dependence of the half-angle of the cone within which the fluorophore rotated (Eq. 4). The errors presented are standard deviations from at least three independent experiments. Experimental conditions were as in Fig. 2.

time suggested that the interactions between neighboring protomers became weaker, and the actin filaments became more flexible, due to the binding of the mDia1-FH2 (see Discussion). It was observed that at a lower actin concentration (5 μM), mDia1-FH2 (>500 nM) could stabilize the structure of actin by binding to the sides of the filaments (19). This stabilization effect required high formin/actin concentration ratios where the formin ''cramps'' interacted with most of the actin protomers in a filament. This property of formins was not observed in this study because the actin concentrations were higher (>20 μM) than that applied in our previous work (5 μM), and thus the formin/actin concentration ratio was <1:4 even at the highest formin concentrations.

The amplitudes of the rotational correlation times (r_1 and r_2) were also found to be formin-concentration-dependent (Fig. 3 *B*, *inset*), indicating that the relative contribution of the two rotational modes to the anisotropy decay was modified by the binding of formin. The value of the R_0 (Eq. 3) was smaller in the presence of mDia1-FH2 than in the absence of it (Fig. 3 *B*). The formin dependence of this parameter was well pronounced below 500 nM mDia1-FH2, where R_0 decreased to 0.265, whereas its value did not change above this concentration. The decrease of the R_0 was attributed to the less rigid protein structure around the bound fluorophore and reflected the loosening effect of mDia1-FH2 on the microenvironment of the Cys^{374}.

Using the amplitudes determined from anisotropy decay experiments, further information could be obtained regarding the microenvironment of Cys^{374}. The theory established by Kinosita and his colleagues (27) assumes that the rotating object characterized by the anisotropy decay measurements can be approximated by the simple geometrical shape. In our experiments, the exact shape of the rotating unit could not be properly determined (see Discussion). We assumed—as an approximation—that the rotating unit is a sphere that undergoes isotropic rotational diffusion. The uncertainty attributed to this assumption probably did not allow the determination of the absolute values of the angular range of the rotations. However, the comparison of estimates obtained from these analyses in the absence and presence of formins were suitable to describe the formin-induced modifications in the structure of the actin filaments. In the model, the symmetry axis of the probe is free to wobble through a limited angular range (within a cone of a semi-angle Θ). Assuming that either the absorption or emission moment is parallel to the cylindrical axis of the fluorophore (38), the two-dimensional angular range, Θ, within which the fluorophore performs wobbling motion could be related to the amplitudes of the

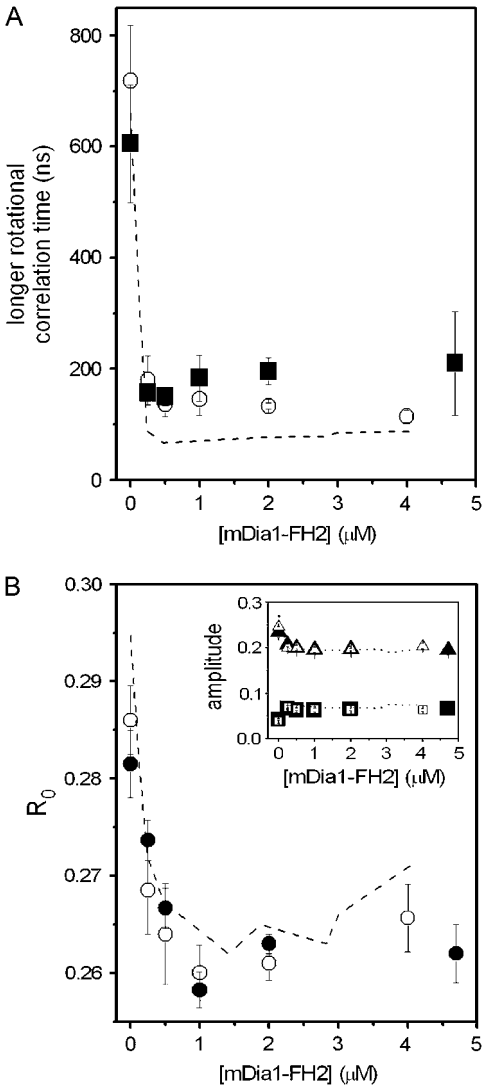

FIGURE 4 The effect of mDia1-FH2 on actin filaments was independent of the actin concentration. (*A*) The mDia1-FH2 concentration dependence of the longer rotational correlation times determined at 30 μM (*open circles*) and 40 μM (*solid squares*) actin concentrations. The dashed line indicates the results with 20 μM actin. (*B*) The mDia1-FH2 concentration dependence of the limiting anisotropy determined at 30 μM (*open circles*) and 40 μM (*solid circles*) actin. Dashed line indicates the results with 20 μM actin from Fig. 3 *C*. (*Inset*) Formin dependence of the amplitudes of the shorter (*squares*) and longer (*triangles*) rotational correlation times at 30 μM (*open symbols*) and 40 μM (*solid symbols*) actin. Dashed line indicates the results with 20 μM actin. The errors presented are standard deviations from at least three independent experiments. Experimental conditions were as in Fig. 2.

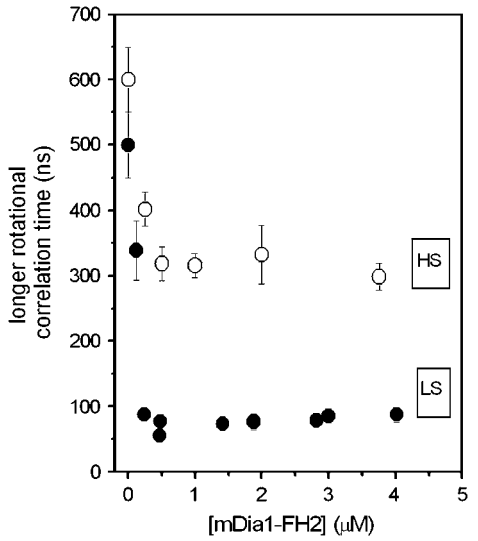

FIGURE 5 The effect of formins on actin filaments was dependent on ionic strength. The figure shows the mDia1-FH2 dependence of the longer rotational correlation times from fluorescence anisotropy decay experiments with 30 μM actin at 0.5 mM $MgCl_2$ and 10 mM KCl (*solid circles*; *LS*) or at 1 mM $MgCl_2$ and 50 mM KCl (*open circles*; *HS*). The errors presented are standard deviations from at least three independent experiments.

two rotational modes resolved in anisotropy decay measurements. The application of this theory also requires that the local motion of the label—reflected by the shorter correlation time—is much faster than the global motion of the protein. This requirement was fulfilled as we observed that the longer rotational correlation times were at least one order of magnitude larger than the shorter ones. The semi-angle (Θ) of the cone within which the IAEDANS at Cys^{374} performs wobbling motion was calculated using Eq. 4. The value of the semi-angle was larger in the presence of mDia1-FH2 than in the absence of it and followed formin-concentration dependence (Fig. 3 *C*) similar to that of the longer rotational correlation times (ϕ_1 in Fig. 3 *A*) and that of the R_0 (Fig. 3 *B*). The greater semi-angles observed in the presence of formin corroborated our conclusions from the formin dependence of the fluorescence lifetimes (Fig. 2 *B*) and R_0 (Fig. 3 *B*) that the microenvironment of the fluorescent probe was more flexible when the filaments were polymerized with mDia1-FH2.

The actin-concentration independence of the formin effect

The fluorescence parameters obtained at 20 μM actin were formin-dependent below ~500 nM mDia1-FH2 and became formin-independent above this concentration (Figs. 2 and 3). In the next set of experiments, we investigated whether it was the formin/actin concentration ratio (1:40), or the total formin concentration (500 nM) that was responsible for this observation. The fluorescence experiments were repeated at 30 μM and 40 μM actin in the presence of various concentrations of mDia1-FH2 (0–5 μM). The longer rotational correlation times, the amplitudes, and the R_0 values are presented in Fig. 4 and indicate that regardless of the applied actin concentration (20–40 μM) the maximum formin-induced effects in the structure of the actin filaments could be observed at ~500 nM mDia1-FH2. The formin-concentration dependence of the fluorescence lifetimes and the calculated semi-angles (Θ) corroborated this conclusion (data not

shown). Above 500 nM the formin-concentration dependence of the fluorescence parameters became negligible. The actin-concentration independence of the smallest formin concentration at which the largest formin effect was observed suggested that the total formin concentration determined the appearance of the maximum formin effect, not the formin/actin concentration ratio.

The ionic-strength dependence of the effects

In our recent study, we found that the effect of formins on the actin filaments depended on the ionic strength (19). Considering this observation, in the work described here we measured the formin-concentration dependence of the rotational correlation times at greater ionic strength (1 mM $MgCl_2$ and 50 mM KCl) as well. In the absence of formins the value of the longer rotational correlation time was independent of ionic strength. The binding of mDia1-FH2 to actin filaments resulted in the decrease of the longer rotational correlation time (Fig. 5). At this higher ionic strength, the formin-induced change of this parameter was only half of that observed at lower salt (0.5 mM $MgCl_2$ and 10 mM KCl). These observations corroborated our previous observation (19) that the formin-induced conformational changes in actin were smaller at higher ionic strength.

DISCUSSIONS

The FH2 fragment of the mammalian formin mDia1 was shown to have long-range allosteric effects on the conformation of actin filaments (19). In this study, we investigated the details of the formin-induced conformational transitions by using time-dependent fluorescence experiments, and tested the mechanism by which formin-binding affects the dynamic properties of the actin filaments.

The correlation times determined in our anisotropy decay measurements cannot be characteristic for the rotation of the whole filament (34,39) and thus their interpretation requires the identification of the parts of the proteins that were characterized by these parameters. There are many motional modes in an actin filament (Fig. 6). The correlation times attributed to the different modes are distributed across a broad time range. Different experimental methods are sensitive to different types of intramolecular motions. The bending motion of the actin filaments was characterized by a correlation time of ~10 ms (40). The correlation times determined by saturation transfer electron paramagnetic resonance fell into the hundreds-of-microseconds timescale (37,41). Transient absorption anisotropy experiments showed that the actin filaments are more flexible in twisting motion than in bending (42) and the correlation times are in the microsecond range. We agree therefore with previous interpretations (32,35,36) that the correlation times of a few hundred nanoseconds in fluorescence anisotropy decay experiments are attributed to restricted segmental motion within the actin

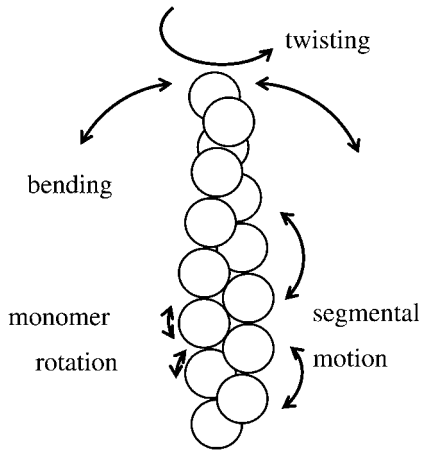

FIGURE 6 A scheme for the interpretation of the various modes of motion of actin. Actin protomers in the filament are symbolized with circles. Arrows indicate the approximate directions in which the actin can move in the different modes.

filaments. The segment characterized by these correlation times can be an actin protomer performing restricted motion in the filament, or a set of a few neighboring protomers with restricted and concerted motion. In this interpretation, the decrease of the correlation time reflects the weakening of the restrictions accompanied by the loosening of the physicochemical links between adjacent protomers in the actin filament.

The rotational correlation times were ~100 ns at 0.5 mM $MgCl_2$ and 10 mM KCl, and ~300 ns at 1 mM $MgCl_2$ and 50 mM KCl in the presence of formin (>500 nM mDia1-FH2). We considered the possibility that mDia1-FH2 induced the partial or complete depolymerization of actin. To exclude this possibility, we measured the rotational correlation time characteristic for actin monomers and found it to be 33 ns. This value was in agreement with previous reports (31,36,43) and was much shorter than the rotational correlation times observed with actin filaments at saturating formin concentrations (~100 ns or ~300 ns (Fig. 5)). This observation suggested that mDia1-FH2 did not depolymerize the actin filaments. Previous observations further corroborated this conclusion. The efficiency of the fluorescence resonance energy transfer between probes on different actin protomers fell into the same range (40–60%) in the presence and absence of mDia1-FH2 (19), which could not be the case if a substantial proportion of the actin was depolymerized. One would expect that the depolymerization effect of an actin-binding compound increases with increasing stoichiometry (up to 1:1). In contrast to this expectation, the longer rotational correlation time was formin-independent in our experiments above the mDia1-FH2 concentration of 500 nM (Figs. 3–5). According to previous results, the mDia1-FH2 fragments did not change the critical concentration of actin (10,19). At high centrifugation speed (400,000 × g), the actin contents of the pellets were independent of the presence

of mDia1-FH2 (19). Considering all these observations, we excluded the possibility that mDia1-FH2 could depolymerize the actin filaments. Based on previous results (13,44), it is likely that the length distribution of actin filaments was similar in the absence and presence of formin at the time of our experiments (see discussion in Bugyi et al. (19)). The observations from the Higgs group suggested that the FH2 domain from mDia1 did not bundle actin filaments (45). According to these considerations the formin-induced decrease of the rotational correlation time was attributed to the loosening effect of mDia1-FH2 on actin filaments.

The largest formin-induced changes in actin filament could be observed in the presence of 500 nM mDia1-FH2. This formin concentration is attributed to 250 nM formin dimers, which are the functional unit of mDia1-FH2 (10,11). We hypothesized that the binding of the mDia1-FH2 fragments to the barbed end of actin filaments was responsible for the long-range allosteric effects on the dynamic properties of the filaments (19). The concentration of the filament ends was estimated as described earlier (46) and was in the range of a few nM. Under the applied conditions, the formin fragments were in large excess over the actin filament barbed ends. If our hypothesis was correct then the formin effect should be actin-concentration independent provided that 1), the formin fragments are in large excess over the filament ends; and 2), the binding of one formin dimer is enough to change the conformation of the whole filament. We confirmed this expectation here by measuring the formin dependence of the anisotropy decay parameters at various actin concentrations (20–40 μM) (Fig. 4). The data set reported here, together with our previous results, showed that the formin effect was independent of actin concentration between 5 μM and 40 μM actin. Considering that mDia1-FH2 binds to the barbed end of actin filaments with an affinity of 20–50 nM (10,13), we concluded that the mDia1-FH2 concentration (250 nM dimer) characteristic for the saturation of the formin effects on actin filaments was required to saturate the formin-binding sites on the barbed ends of actin filaments.

The rotational correlation times were formin-concentration independent above 500 nM mDia1-FH2 (Figs. 3 *A* and 4 *A*), indicating that the binding of formin to a barbed end could modify the conformation of the entire filament. The smallest formin/actin concentration ratio was achieved at 250 nM formin (dimers) and at 40 μM actin. Under these conditions each mDia1-FH2 dimer bound to a filament of at least 160 actin protomers. We concluded therefore that one mDia1-FH2 dimer could modify the conformation of at least 160 actin protomers in an actin filament by long-range allosteric interactions. Considering the finite affinity of mDia1-FH2 for actin and the annealing activity of actin filaments, it is likely that $>$160 protomers were affected by one mDia1-FH2 molecule.

Similar long range allosteric interactions were observed previously in actin filaments (47–52). Gelsolin binding to the filament ends induced long-range allosteric interactions (52) and altered the conformation of whole actin filaments (50). These observations together with our present findings indicate that the structure of actin filaments and the interprotomer connections between neighboring protomers allow the propagation of the conformational changes induced at the ends to distant locations along the actin filaments. It was proposed that the conformational heterogeneity of the filaments is correlated with the regulatory effects of actin-binding proteins (51), and due to their inherent properties actin filaments can serve as informational channels in the regulation of the actin cytoskeleton (19,53).

CONCLUSIONS

We described in this study details of the formin-induced conformational changes in actin filaments. The binding of mDia1-FH2 to actin filaments resulted in a looser protein structure in the microenvironment of the Cys^{374} in the filaments (Figs. 2 *B* and 3, *B* and *C*). In accordance with this effect, the overall flexibility of the actin filaments was also increased by formins (Fig. 3 *A*), probably due to the weakening of the interaction between neighboring protomers. The formin effect was dependent on ionic strength (Fig. 5) in a manner similar to that described in a recent publication (19). The formin concentration required for the full formin effect ($\sim$250 nM dimer) was independent of actin concentration (Fig. 4), in agreement with the model in which formin binding to the barbed end of actin filaments increases the flexibility of the entire filament. The analyses of the formin effect at various formin/actin concentration ratios showed that at least 160 actin protomers were affected by the binding of a single formin dimer to the barbed end of a filament.

This work was supported by the Hungarian Academy of Sciences and by grants from the Hungarian National Research Foundation (OTKA grant No. K 60186 (M.N.), K 60968 (B.S.) and D048545 (G.H.)). G.H. is supported by the János Bolyai Research Fellowship of the Hungarian Academy of Sciences. M.N. holds a Wellcome Trust International Senior Research Fellowship in Biomedical Sciences.

REFERENCES

1. Wallar, B. J., and A. S. Alberts. 2003. The formins: active scaffolds that remodel the cytoskeleton. *Trends Cell Biol.* 13:435–446.
2. Wasserman, S. 1998. FH proteins as cytoskeletal organizers. *Trends Cell Biol.* 8:111–115.
3. Evangelista, M., D. Pruyne, D. C. Amberg, C. Boone, and A. Bretscher. 2002. Formins direct Arp2/3-independent actin filament assembly to polarize cell growth in yeast. *Nat. Cell Biol.* 4:32–41.
4. Feierbach, B., F. Verde, and F. Chang. 2004. Regulation of a formin complex by the microtubule plus end protein tea1p. *J. Cell Biol.* 165:697–707.
5. Moseley, J. B., I. Sagot, A. L. Manning, Y. Xu, M. J. Eck, D. Pellman, and B. L. Goode. 2004. A conserved mechanism for Bni1- and mDia1-induced actin assembly and dual regulation of Bni1 by Bud6 and profilin. *Mol. Biol. Cell.* 15:896–907.

6. Feierbach, B., and F. Chang. 2001. Roles of the fission yeast formin for3p in cell polarity, actin cable formation and symmetric cell division. *Curr. Biol.* 11:1656–1665.
7. Yasuda, S., F. Oceguera-Yanez, T. Kato, M. Okamoto, S. Yonemura, Y. Terada, T. Ishizaki, and S. Narumiya. 2004. Cdc42 and mDia3 regulate microtubule attachment to kinetochores. *Nature*. 428:767–771.
8. Zigmond, S. H. 2004. Formin-induced nucleation of actin filaments. *Curr. Opin. Cell Biol.* 16:99–105.
9. Pruyne, D., M. Evangelista, C. Yang, E. Bi, S. Zigmond, A. Bretscher, and C. Boone. 2002. Role of formins in actin assembly: nucleation and barbed-end association. *Science*. 297:612–615.
10. Li, F., and H. N. Higgs. 2003. The mouse formin mDia1 is a potent actin nucleation factor regulated by autoinhibition. *Curr. Biol.* 13: 1335–1340.
11. Shimada, A., M. Nyitrai, I. R. Vetter, D. Kuhlmann, B. Bugyi, S. Narumiya, M. A. Geeves, and A. Wittinghofer. 2004. The core FH2 domain of diaphanous-related formins is an elongated actin binding protein that inhibits polymerization. *Mol. Cell.* 13:511–522.
12. Xu, Y., J. B. Moseley, I. Sagot, F. Poy, D. Pellman, B. L. Goode, and M. J. Eck. 2004. Crystal structures of a formin homology-2 domain reveal a tethered dimer architecture. *Cell.* 116:711–723.
13. Romero, S., C. Le Clainche, D. Didry, C. Egile, D. Pantaloni, and M. F. Carlier. 2004. Formin is a processive motor that requires profilin to accelerate actin assembly and associated ATP hydrolysis. *Cell.* 119:419–429.
14. Wallar, B. J., B. N. Stropich, J. A. Schoenherr, H. A. Holman, S. M. Kitchen, and A. S. Alberts. 2006. The basic region of the diaphanous-autoregulatory domain (DAD) is required for autoregulatory interactions with the diaphanous-related formin inhibitory domain. *J. Biol. Chem.* 281:4300–4307.
15. Nezami, A. G., F. Poy, and M. J. Eck. 2006. Structure of the autoinhibitory switch in formin mDia1. *Structure*. 14:257–263.
16. Lammers, M., R. Rose, A. Scrima, and A. Wittinghofer. 2005. The regulation of mDia1 by autoinhibition and its release by Rho*GTP. *EMBO J.* 24:4176–4187.
17. Schonichen, A., M. Alexander, J. E. Gasteier, F. E. Cuesta, O. T. Fackler, and M. Geyer. 2006. Biochemical characterization of the diaphanous autoregulatory interaction in the formin homology protein FHOD1. *J. Biol. Chem.* 281:5084–5093.
18. Li, F., and H. N. Higgs. 2005. Dissecting requirements for autoinhibition of actin nucleation by the formin, mDia1. *J. Biol. Chem.* 280:6986–6992.
19. Bugyi, B., G. Papp, G. Hild, D. Lorinczy, E. M. Nevalainen, P. Lappalainen, B. Somogyi, and M. Nyitrai. 2006. Formins regulate actin filament flexibility through long-range allosteric interactions. *J. Biol. Chem.* 281:10727–10736.
20. Feuer, G., F. Molnár, E. Pettkó, and F. B. Straub. 1948. Studies on the composition and polymerisation of actin. *Hung. Acta Physiol.* 1:150–163.
21. Spudich, J. A., and S. Watt. 1971. The regulation of rabbit skeletal muscle contraction. I. Biochemical studies of the interaction of the tropomyosin-troponin complex with actin and the proteolytic fragments of myosin. *J. Biol. Chem.* 246:4866–4871.
22. Houk, T. W., Jr., and K. Ue. 1974. The measurement of actin concentration in solution: a comparison of methods. *Anal. Biochem.* 62:66–74.
23. Elzinga, M., J. H. Collins, W. M. Kuehl, and R. S. Adelstein. 1973. Complete amino-acid sequence of actin of rabbit skeletal muscle. *Proc. Natl. Acad. Sci. USA.* 70:2687–2691.
24. Miki, M., C. G. dos Remedios, and J. A. Barden. 1987. Spatial relationship between the nucleotide-binding site, Lys-61 and Cys-374 in actin and a conformational change induced by myosin subfragment-1 binding. *Eur. J. Biochem.* 168:339–345.
25. Hudson, E. N., and G. Weber. 1973. Synthesis and characterization of two fluorescent sulfhydryl reagents. *Biochemistry.* 12:4154–4161.
26. Belford, G. G., R. L. Belford, and G. Weber. 1972. Dynamics of fluorescence polarization in macromolecules. *Proc. Natl. Acad. Sci. USA.* 69:1392–1393.
27. Kinosita, K., Jr., S. Kawato, and A. Ikegami. 1977. A theory of fluorescence polarization decay in membranes. *Biophys. J.* 20:289–305.
28. Alcala, J. R., E. Gratton, and F. G. Prendergast. 1987. Interpretation of fluorescence decays in proteins using continuous lifetime distributions. *Biophys. J.* 51:925–936.
29. Alcala, J. R., E. Gratton, and F. G. Prendergast. 1987. Fluorescence lifetime distributions in proteins. *Biophys. J.* 51:597–604.
30. Alcala, J. R., E. Gratton, and F. G. Prendergast. 1987. Resolvability of fluorescence lifetime distributions using phase fluorometry. *Biophys. J.* 51:587–596.
31. Nyitrai, M., G. Hild, J. Belagyi, and B. Somogyi. 1997. Spectroscopic study of conformational changes in subdomain 1 of G-actin: influence of divalent cations. *Biophys. J.* 73:2023–2032.
32. Miki, M., P. Wahl, and J. C. Auchet. 1982. Fluorescence anisotropy of labelled F-actin. Influence of Ca2+ on the flexibility of F-actin. *Biophys. Chem.* 16:165–172.
33. Hild, G., M. Nyitrai, J. Belagyi, and B. Somogyi. 1998. The influence of divalent cations on the dynamic properties of actin filaments: a spectroscopic study. *Biophys. J.* 75:3015–3022.
34. Tawada, K., P. Wahl, and J. C. Auchet. 1978. Study of actin and its interactions with heavy meromyosin and the regulatory proteins by the pulse fluorimetry in polarized light of a fluorescent probe attached to an actin cysteine. *Eur. J. Biochem.* 88:411–419.
35. Miki, M., P. Wahl, and J. C. Auchet. 1982. Fluorescence anisotropy of labeled F-actin: influence of divalent cations on the interaction between F-actin and myosin heads. *Biochemistry.* 21:3661–3665.
36. Ikkai, T., P. Wahl, and J. C. Auchet. 1979. Anisotropy decay of labelled actin. Evidence of the flexibility of the peptide chain in F-actin molecules. *Eur. J. Biochem.* 93:397–408.
37. Hegyi, G., L. Szilagyi, and J. Belagyi. 1988. Influence of the bound nucleotide on the molecular dynamics of actin. *Eur. J. Biochem.* 175:271–274.
38. Lipari, G., and A. Szabo. 1980. Effect of librational motion on fluorescence depolarization and nuclear magnetic resonance relaxation in macromolecules and membranes. *Biophys. J.* 30:489–506.
39. Kawamura, M., and K. Maruyama. 1970. Electron microscopic particle length of F-actin polymerized in vitro. *J. Biochem. (Tokyo).* 67:437–457.
40. Fujime, S., and S. Ishiwata. 1971. Dynamic study of F-actin by quasielastic scattering of laser light. *J. Mol. Biol.* 62:251–265.
41. Thomas, D. D., J. C. Seidel, and J. Gergely. 1979. Rotational dynamics of spin-labeled F-actin in the sub-millisecond time range. *J. Mol. Biol.* 132:257–273.
42. Mihashi, K., H. Yoshimura, T. Nishio, A. Ikegami, and K. Kinosita, Jr. 1983. Internal motion of F-actin in 10^{-6}–10^{-3} s time range studied by transient absorption anisotropy: detection of torsional motion. *J. Biochem. (Tokyo).* 93:1705–1707.
43. Miki, M., and P. Wahl. 1985. Fluorescence energy transfer between points in G-actin: the nucleotide-binding site, the metal-binding site and Cys-373 residue. *Biochim. Biophys. Acta.* 828:188–195.
44. Andrianantoandro, E., L. Blanchoin, D. Sept, J. A. McCammon, and T. D. Pollard. 2001. Kinetic mechanism of end-to-end annealing of actin filaments. *J. Mol. Biol.* 312:721–730.
45. Harris, E. S., I. Rouiller, D. Hanein, and H. N. Higgs. 2006. Mechanistic differences in actin bundling activity of two mammalian formins, FRL1 and mDia2. *J. Biol. Chem.* 281:14383–14392.
46. Kovar, D. R., J. R. Kuhn, A. L. Tichy, and T. D. Pollard. 2003. The fission yeast cytokinesis formin Cdc12p is a barbed end actin filament capping protein gated by profilin. *J. Cell Biol.* 161:875–887.
47. Oosawa, F. 1972. Dynamic properties of F-actin and the thin filament. *Nippon Seirigaku Zasshi.* 34:96–97.
48. Drewes, G., and H. Faulstich. 1993. Cooperative effects on filament stability in actin modified at the C-terminus by substitution or truncation. *Eur. J. Biochem.* 212:247–253.
49. Muhlrad, A., P. Cheung, B. C. Phan, C. Miller, and E. Reisler. 1994. Dynamic properties of actin. Structural changes induced by beryllium fluoride. *J. Biol. Chem.* 269:11852–11858.

50. Orlova, A., E. Prochniewicz, and E. H. Egelman. 1995. Structural dynamics of F-actin: II. Cooperativity in structural transitions. *J. Mol. Biol.* 245:598–607.

51. Orlova, A., A. Shvetsov, V. E. Galkin, D. S. Kudryashov, P. A. Rubenstein, E. H. Egelman, and E. Reisler. 2004. Actin-destabilizing factors disrupt filaments by means of a time reversal of polymerization. *Proc. Natl. Acad. Sci. USA.* 101:17664–17668.

52. Prochniewicz, E., Q. Zhang, P. A. Janmey, and D. D. Thomas. 1996. Cooperativity in F-actin: binding of gelsolin at the barbed end affects structure and dynamics of the whole filament. *J. Mol. Biol.* 260: 756–766.

53. Visegrády, B., D. Lőrinczy, G. Hild, B. Somogyi, and M. Nyitrai. 2005. A simple model for the cooperative stabilisation of actin filaments by phalloidin and jasplakinolide. *FEBS Lett.* 579:6–10.